Spectroscopy of Inhibited Counterflow Diffusion Flames

R. G. Daniel, K. L. McNesby, R. R. Skaggs, P. Sagear, and A. W. Miziolek
U.S. Army Research Laboratory
Weapons and Materials Research Directorate
AMSRL - WM - PC
Aberdeen Proving Ground, MD 21005-5066

ABSTRACT

As part of the continuing effort to find an effective, yet safe, replacement compound for the commonly used halon fire suppression agents, we have begun a study of reduced pressure counterflow diffusion flames inhibited with iron pentacarbonyl ($Fe(CO)_5$). Iron pentacarbonyl has been shown to be a very effective fire suppression agent in small quantities, but there is little understanding to the mechanism of its activity. Unfortunately, $Fe(CO)_5$ is highly toxic and thus cannot be used in occupied spaces. The goal of this study is to understand the mechanism by which $Fe(CO)_5$ inhibits flames by coupling experimental measurements with computer modeling of diffusion flames. Presented here are results from the spectroscopic examination of uninhibited and inhibited counterflow diffusion flame using emission spectroscopy of active flame species at reduced pressure. The species studied include OH, CH, C_2, and iron and iron containing compounds. This project is part of the Next Generation Fire Suppression Technology Program (NGFSTP).
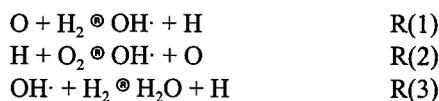
INTRODUCTION

Halogenated fire extinguishment agents, such as Halon 1301 (CF_3Br) and Halon 1211 (CF_2ClBr), continue to be some of the most effective fire extinguishing agents known. However, due to their linkage to stratospheric ozone depletion their use has been greatly restricted by international agreement [1]. Many replacement agents are still highly halogenated, i.e. FM-200 (C_3F_7H), and while effective, often require greater quantities to be used in fire fighting applications [2]. Other replacement compounds, although proven effective, suffer from ozone depletion potentials which are unacceptable (CF_3I) [3]. The search for effective, non-toxic, environmentally benign replacement agents thus continues.

One compound which has been shown, through experimental and modeling studies [4,5], to be extremely effective in small concentrations is $Fe(CO)_5$, which also suffers from high toxicity [6]. This project is designed to understand the mechanism of fire suppression/extinguishment of this superagent type compound. This understanding should lead to the design and development of new agents which meet all the criteria for a replacement compound. The study presented here utilizes a counterflow diffusion burner capable of being operated at either reduced or elevated pressures. We will spectroscopically map flame species via emission spectroscopy, as well as map flame temperatures with traditional thermocouple techniques, in flames at several pressures and inhibited with several different agents.
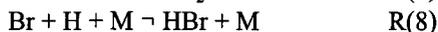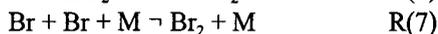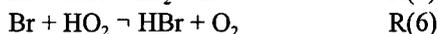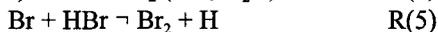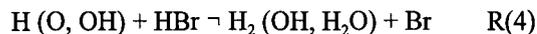
BACKGROUND

The combustion process of any fuel is the combination of many elementary reactions of many different chemical species interacting with the fluid dynamics of the system. This complexity can be reduced to a few key reactions which are primarily responsible for the propagation of the overall chemistry. When a chemical agent is introduced which interrupts this propagation, the flame can be extinguished or suppressed. The principal radical reactions for hydrocarbon combustion in air are [7] :

$$O + H_2 \circledR OH\cdot + H \qquad R(1)$$
$$H + O_2 \circledR OH\cdot + O \qquad R(2)$$
$$OH\cdot + H_2 \circledR H_2O + H \qquad R(3)$$

These three reactions form the major chain-branching mechanism for flame propagation, with R(2) being the
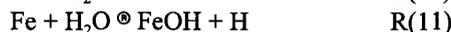
dominant chain-branching reaction in the flame[8] and the primary channel for oxygen consumption.

When an inhibiting agent is introduced to the flame, chemical inhibition is believed to arise from the lowering of the concentration of radicals through scavenging reactions and/or physical inhibition arises from an absorption of heat energy due to the heat capacity of the agent. A scavenging reaction is defined as a process that converts reactive radicals to stable species and/or less reactive radicals [9] . Halon 1301 (CF_3Br) acts primarily as a chemical inhibitor via the follwing scavenging reactions [10]:

$$H\ (O,\ OH) + HBr \neg H_2\ (OH,\ H_2O) + Br \qquad R(4)$$
$$Br + HBr \neg Br_2 + H \qquad R(5)$$
$$Br + HO_2 \neg HBr + O_2 \qquad R(6)$$
$$Br + Br + M \neg Br_2 + M \qquad R(7)$$
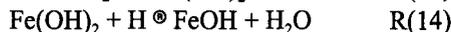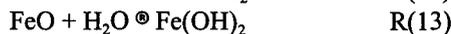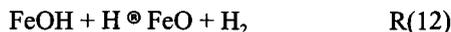$$Br + H + M \neg HBr + M \qquad R(8)$$

These reactions remove the reactive radicals OH and HO_2 and regenerate the active species HBr, which then repeats the cycle. This catalytic activity is why CF_3Br is so effective as an inhibiting agent.

Flame suppression by metal containing agents, such as iron pentacarbonyl ($Fe(CO)_5$), is often assumed to occur by three competing suppression pathways: metal-oxygen-oxygen monomers form and cause homogeneous free radical removal, metal containing particles form and undergo heterogeneous free radical recombination on their surfaces, and heat absorption due to agent decomposition. Reinelt et al. [11] have suggested the following mechanism for the inhibition activity of $Fe(CO)_5$. Iron pentacarbonyl initially undergoes thermal decomposition and then the free iron reacts with oxygen and water to produce scavenging iron oxides.

$$Fe(CO)_5 \circledR Fe + 5\ CO \qquad R(9)$$
$$Fe + O_2 \circledR FeO + O \qquad R(10)$$
$$Fe + H_2O \circledR FeOH + H \qquad R(11)$$

The iron oxides then promote the catalytic recombination of H atoms to hydrogen (H_2).

$$FeOH + H \circledR FeO + H_2 \qquad R(12)$$
$$FeO + H_2O \circledR Fe(OH)_2 \qquad R(13)$$
$$Fe(OH)_2 + H \circledR FeOH + H_2O \qquad R(14)$$

The removal of the H atoms inhibits the chain-branching reaction R(2) which reduces the overall rate of combustion. In flames, iron oxides have been observed to form condensed phase particles that are highly luminous[12] . This observation also lends support to the heterogeneous inhibition mechanism mentioned above.

As illustrated above, the proposed inhibition mechanism is quite complex, involving both homogeneous and heterogeneous catalytic cycles that result in the extinguishment of the flame. Presented here are results from the first portion of this study, in which the flame temperature is measured with Pt/10%Pt-Rh thermocouples and the emission of the neat and inhibited flames is recorded. The next statges of the study will include the mapping of species concentration by laser induced fluorescence (LIF), planar laser induced fluorescence (PLIF), tunable diode laser (TDL) absorption spectroscopy, near-IR TDL spectroscopy, and a computational modeling study of the flames.

EXPERIMENTAL

The counterflow diffusion burner apparatus consists principally of three components: a gas handling manifold, the burner chamber with vacuum system, and the analytic equipment. Each component will be outline briefly in the following paragraphs. The oxidizer and fuel gases are prepared in the desired proportions, with or without inhibiting agent, by the gas manifold before entering the burner chamber. The fuel usually enters through the bottom head and the oxidizer from the top. The oxidizer and fuel mix between the two heads and there the flame front is supported. Unburnt gases and combustion products are exhausted from the chamber through eight ports, two by each window, by a high volume vacuum pump.

FLOW CONTROL SYSTEM

The gas handling manifold consists of a network of Tylan General flow controllers originally designed to produce a flow velocity of 100 cm/s from both heads in the pressure range of 0.5 torr to 2 atm. We do not utilize this high flow rate due to the excessive amounts of gases required to maintain these flows. Each arm of the manifold has two flow controllers installed, a high flow and medium flow, and selected via valves. The manifold also allows for the inhibitor to be introduced to either the fuel flow or the oxidizer flow. The flow controllers are electronically operated via two mass flow control boxes, with one channel operating a single gas being introduced to the system. The gases normally introduced are fuel (typically methane), nitrogen (to manufacture air, as a diluent, as a inhibitant carrier, and as a window buffer), oxygen, and inhibitant. The manifold has solenoid controlled safety valves, normally closed, as the final output valve to the system. No gas is allowed to flow in the event of a power outage or the pressing of an emergency cut-off switch.

The inhibitant is introduced as a gas when possible. One arm of the gas manifold is used to introduce argon and Halon 1301, both of which are gaseous at room temperature. Iron pentacarbonyl is a liquid at room temperature with a vapor pressure of 19.4 mm/Hg at 15 °C. To introduce the $Fe(CO)_5$ to the system, nitrogen is bubbled through a flask, immersed in a constant temperature bath, containing the liquid. The nitrogen is introduced via one of the gas manifold flow controllers. The output of the bubler passes through a rotameter to measure precisely how much of the saturated vapor is entering the gas stream. We have minimized the distance traveled between the bubbler and the burner head to reduce the amount of $Fe(CO)_5$ which decomposes rapidly in air.

THE BURNER SYSTEM

The combustion chamber is a six armed stainless steel cross with the four horizontal arms being ten inches in diameter and the two vertical arms being twelve inches in diameter. The opposed jet burners (Figure 1) are mounted in the vertical arms, with each head having two axis of motion under computer control. The active burner area is three inches in diameter. The gas and cooling water are fed to the head via stainless tubing. Gases introduced first impinge on a deflector plate and then expand through the porous plate to a second chamber also sealed by a porous plate. This second porous plate opens to the combustion chamber.

Optical access to the chamber is provided on the four vertical arms of the chamber where four inch diameter windows are mounted. There are also four additional ports in the horizontal plane, each located between two of the window arms. These ports serve as access for pressure monitoring, thermocouple manipulation, and electrical access. Also mounted on top and bottom of each window arm are vacuum ports to remove the combustion gases. These eight ports are joined to a single two inch I.D. tube which feeds the gas to a scrubber mounted on a high volume vacuum pump. The scrubbed exhaust gases are then vented to the atmosphere.

ANALYTIC EQUIPMENT

The combustion chamber is located between two optical tables which support the majority of the analytical equipment used in characterizing the flames under study.

The thermocouple is constructed from Pt and 10%Pt/Rh wires which are .008 inch in diameter or smaller. The thermocouple wires were used with a refractory coating of magnesium oxide (MgO) in both the uninhibited flames and inhibited flames. This was produced by making a slurry of magnesium perchlorate ($Mg(ClO_4)_2$), swabbing the wires with the slurry, and then passing the coated wires through the flame of a propane torch. The flame drives off the moisture, producing the MgO coating[13].

The emission data is collected using a two dimensional CCD camera attached to a monochromator. A 0.5 meter focal length lens is use dto image the center of the flame on the input slits of a Spex 500 mm monochromator. Mounted on the output of the monochromator is a Princeton Instruments two dimensional CCD camera. The camera is operated with a model ST 138 controller and PG200 Pulse Generator. The active array area is 576 x 384 pixels. This active pixel area produces an image which is 11.1 mm in height and approximately 20 nm wide. The images obtained thus contain both spectral information and spatial information. A software package supplied by Princeton Instruments allows the images to be separated into both of these components, binning the individual pixels according to spatial dimension or spectral region.

EXPERIMENTAL CONDITIONS

In order to understand the complexities of a flame, inhibited or unihibited, one must reduce it to as simple a system as possible. In the past we examined low pressure premixed flames[14] which simplified the modeling of the system and also produced a flame which was readily characterized spectroscopically by expanding the luminous zone of the flame.

In this study we are examining counterflow diffusion flames at reduced pressure conditions. Due to the physical characteristics of the flames at the pressures examined, the experimental conditions vary flame to flame so that the flames are stable enough to be examined physically and spectroscopically. The flame pressures at which experiments were performed are 50 torr and 300 torr. Attempts to study a flame at true atmsopheric pressure (760 torr) with the present gas flow rates was unsuccessful due to instability in the flame. Table 1 lists the conditions of each of the flames studied, with flow rates given in standard liters per minute (slm). The buffer flow was the flow rate of nitrogen input around the windows to prevent condensation of the combustion gases on the windows. This gas was part of the total gas load to produce the reported pressures.

Table 1. List of experimental conditions for the three flames used in the present study.

Flame Pressure	Fuel Flow	Oxidizer Flow	Buffer Flow
50 torr	3.0 slm CH_4	1.1 slm O_2 3.9 slm N_2	1.5 slm N_2
300 torr	6.0 slm CH_4	2.2 slm O_2 7.8 slm N_2	3.0 slm N_2
700 torr	1.0 slm CH_4 5.8 slm N_2	2.0 slm O_2 6.0 slm N_2	1.5 slm N_2

RESULTS AND DISCUSSION

We have concentrated on the two reduced pressure flames for the main body of work for ease of operation, to minimize damage to the experimental apparatus, and to facilitate comparison to the ongoing modeling work. Most of the results will thus be on the comparison between these two flames and between different inhibitors in the

same flame. Both CF_3Br and $Fe(CO)_5$ offer challenges as additives. $Fe(CO)_5$ forms particulates in the flame, which while they may aid in the reduction of flame temperature by conductive heat loss, also coat the interior of the combustion chamber, vacuum lines, and ultimately the high volume vacuum pump. CF_3Br generates significant amounts of HF. Hydrofluoric acid, while toxic, is also highly corrosive, and it is the corrosivity which complicates the experimental study of fluorinated additives.

As mentioned above, $Fe(CO)_5$ generates particulates in the flames. These particulates then deposit on any cool surface available to them, which is primarily the cooled burner heads. Samples of these particles have been collected and analyzed using a scanning electron microscope (SEM) and X-ray fluorescence (XRF) to identify the molecular composition. The particulate material is a ruddy orange color in appearance, typical of iron containing compounds. Particles were collected from the upper (oxidizer) burner head and also from a thermocouple which had been used to record temperatures in a doped flame. The XRF showed the composition of the particles to be iron and oxygen, although an exact ratio was not determined. This was the expected result, the $Fe(CO)_5$ decomposes and some of the iron combines to form Fe_xO_y particles. The SEM photographs showed the size of the particles ranged from 1 to 10 microns, with most being on the order of 1 - 2 microns. The effectiveness of a 2 micron particle involved in heat conduction is being explored as a possible component of the overall suppression mechanism of iron pentacarbonyl, although that determination has not been finalized.

Dopant	50 Torr	300 Torr
Argon	400 cc/min	3.0 slm
CF_3Br	120 cc/min	120 cc/min
$Fe(CO)_5$	15 cc/min	15 cc/min

For each of the flames studied, a scan of the full spectrum was taken from 250 to 1100 nm. Portions of this spectrum were recorded with the CCD for further analysis. The position of the flame relative to the oxidizer burner head, and intensity of the molecular spectra varied with dopant identity. Table 2 lists the dopant level for the 50 and 300 torr flames. The spectra recorded contains both wavelength dispersion and physical height. The spatial distibution of the OH emission between the burner heads is shown in Figure 2 for both the 50 and 300 torr flames. In the 50 torr flame, the addition of argon, which acts as an inert diluent, shifts the flame position away from the oxidizer head. This is indicative of a change in the position of the stoichiometric region supporting the flame, caused by a change in the momentum balance of the gas flows. The CF_3Br also appears to shift the OH emission peak away from the oxidizer head by a small amount. There is virtually no change in the position of the emission intensity upon the addition of the $Fe(CO)_5$. This is not the case in the 300 torr flame. The argon shifting the flame front away from the oxidizer head can be atributed to the dilution of the air, as we increase the total flow from the oxidizer head by 30%. Both the $Fe(CO)_5$ and CF_3Br move the flame front closer to the oxidizer head. This may be an indication of their radical scavenging ability. As the H and OH population is depleted early in the oxidizer flow, the flame must reposition itself to remain supported on the remaining radical population. Similar effects have been observed for both the C_2 emission at 473.7 nm and the CH emission at 431.4 nm.

The addition of an iron containing compound to the flame does change the molecular emission spectra through the addition of atomic iron lines and of iron species such as FeO and FeOH. Iron has a very rich line spectrum which spans from the near ultraviolet to the near infrared regions. The most intense lines lie toward the blue end of the spectrum. These lines greatly alter the spatial distribution of the emission intensity, but also lend key insight into the area of activity of the $Fe(CO)_5$ within the flame. Figure 3 illustrates this effect. The cross section (Figure 3a) of the emission of CH has an additional region of emission intensity closer to the oxidizer head which is missing in the neat and other two doped flames. Some of this has been identified as iron lines not present in the neat flame, shown in Figure 3b. This spatial mapping shows that the iron pentacarbonyl has at least started to decompose prior to the luminous flame region. This change in intensity is also observed visually, as a second bright

luminous zone appears nearer the oxidizer head in the 300 torr flame upon the addition of the iron pentacarbonyl. In Figure 4 is shown both the spectrum of FeOH at 352 nm and the spatial distribution of the FeOH in the two flames studied. The spatial distribution of the FeOH for the two flames is very similar, with just an off-set due to the flame position relative to the oxidizer burner head. This suggests a similarity in the chemical activity at the two reduced pressures.

We have also examined the response of flame temperature to the addition of CF_3Br and $Fe(CO)_5$, and the effect of flame temperature on the position and intensity of the emission of OH. Shown in Figure 5 are plots of flame temperature for the 50 and 300 torr flame when undoped and when doped with $Fe(CO)_5$. The $Fe(CO)_5$ lowered the peak temperature by over 300 °C at both pressures. This temperature change was not observed with the addition of CF_3Br, but the flame temperature remained essentially superimposable upon the neat flame temperature, independent of the amount of agent added.

CONCLUSIONS

We are continuing to study the effects of iron pentacarbonyl on counterflow diffusion flames at atmospheric and reduced pressure to elucidate the suppression mechanism of this prototypical superagent. The next phase of this study, currently underway, is to examine species concentrations using laser induced fluorescence. The species to be studied are O, H, and OH. We will also examine O, CH_4, H_2O, and HF (when produced) using near infrared absorption spectroscopy. The study will also address different fuels. All of the results will be compared with the modeling study of diffusion flames performed in a collaborative effort.

ACKNOWLEDGEMENTS

REFERENCES

1. Fourth Meeting of the Parties to the Montreal Protocol on Substances that Deplete the Ozone Layer, 23-25 Nov 1992, Copenhagen. Doc.no. UNEP/OzL.Pro.4/15 (Nairobi:UNEP, 1992),32. The full text of the London and Copenhagen amendments to the Montreal Protocol on Substances that Deplete the Ozone Layer, with the Montreal Protocol attached as an appendix can be found at gopher://gopher.law.cornell.edu/00/foreign/fletcher/MONTREAL-1992.txt.

2. Moore, T. A., Martinez, A., and Tapscott, R. E., *Proceedings of theHalon Options Technical Working Conference*, May 1997, p388 - 95.

Williams, B. A., Fleming, J. W., and Sheinson, R. S., *Proceedings of theHalon Options Technical Working Conference*, May 1997, p31 - 42.

3. Solomon, S., Burkholder, J. B., Ravishankara, A. R., and Garcia, R. R., *Journal of Geophysical Research*, **99**, p 20929-935, 1994.

Connell, P. S., Kinnison, D. E., Bergman, D. J., Patten, K. O., Wuebbles, D. J., Daniel, R. G., Williamson, C. K., Miziolek, A. W., and Huie, R. E., *Proceedings of theHalon Options Technical Working Conference*, May 1996, p585 - 98.

4. Lask,G., and Wagner, H.G., *Eighth Symposium (Interntional) on Combustion*, The Combustion Institute, Williams and Wilkens, p432 - 38, 1962.

5. Bonne, U., Jost, W., and Wagner, H.G., *Fire Research Abstracts and Reviews,* 4, p 6-18, 1962.

6. Pitts, W. M., Nyden, M. R., Gann, R. G., Mallard, W. G., and Tsang, W., NIST Technical Note 1279, U. S. Department of Commerce, Chapter 3, Section J., p73 - 4.

7. Day, M. J., Dixon-Lewis, G., and Thompson, K., *Proceedings of the Royal Society (London)*, **A330**, p199, 1972.

8. McKinnon, J. T., and Howard, J. B., *Combustion Science and Technology*, **74**, p 159 - 73, 1990.

9. Senkan, S. M., in Detoxification of Hazardous Waste: Combustion Characteristics of Chlorinated Hydrocarbon, J. H. Exner, ed., Ann Arbor Science, p 61 - 92, 1992.

10. Biordi, J. C., Lazzara, C. P., and Papp, J. F., in Halogenated Fire Suppressants, R. G. Gann, ed., ACS Symposium Series 16, p 256 - 94, 1975.

11. Reinelt, D., and Linteris, G. T., *Twentysixth Symposium (International) on Combustion*, The Combustion Institute, Pittsburgh, in press, 1996.

12. Hastie, J. W., in High Temperature Vapors, Academic Press, New York, p 335 - 57, 1975.

13. Kent, J. H., *Combust. Flame*, **14**, p 279, 1970.

14. Daniel, R. G., McNesby, K. L., and Miziolek, A. W., *Applied Optics*, **35**, p 4010, 1996.